Research paper

Effective palynological diversity indices for reconstructing angiosperm diversity in China

Yuxuan Jiang [a, b], Fuli Wu [a, *], Xiaomin Fang [a, b], Haitao Wang [a, c], Yulong Xie [a, d], Cuirong Yu [a, b]

[a] State Key Laboratory of Tibetan Plateau Earth System, Environment and Resources (TPESER), Institute of Tibetan Plateau Research, Chinese Academy of Sciences, Lincui Road 16, Beijing 100101, China
[b] University of Chinese Academy of Sciences, Beijing 100101, China
[c] Key Laboratory of Ecological Safety and Sustainable Development in Arid Lands, Northwest Institute of Eco-Environment and Resources, Chinese Academy of Sciences, Lanzhou 730000, China
[d] Key Laboratory of Palaeobiology and Petroleum Stratigraphy, Nanjing Institute of Geology and Palaeontology, Chinese Academy of Sciences, Nanjing 210008, China

ARTICLE INFO

ABSTRACT

The utilization of palynological data for plant diversity reconstructions offers notable advantages in addressing the discontinuity of plant fossils in the stratigraphic record. However, additional studies of modern processes are required to validate or refine the accuracy of diversity results obtained from palynological data. In this study, we used a modern pollen dataset of China to compare the accuracy of plant diversity reconstructions using five different palynological diversity indices (i.e., the pollen species number, Berger−Parker index, Simpson diversity index, Hill index, and Shannon−Wiener index) over a large spatial scale. We then identified climate factors that are most strongly correlated with these patterns of plant diversity. We found that the index that most accurately reflects plant diversity is the Shannon−Wiener index. Our analyses indicated that the most effective indices at reflecting plant diversity are the Shannon−Wiener index and Berger−Parker index. Numerical analysis revealed that palynological diversity (measured using the Shannon−Wiener index) was strongly correlated with climatic parameters, in particular average temperature in the coldest month and annual precipitation, suggesting these factors may be primary determinants of plant diversity distribution. We also found that a threshold value of the normalized Shannon−Wiener index (NH = 0.4) approximately aligns with the contour line specifying 400 mm annual precipitation, serving as a rudimentary indicator for assessing plant diversity in arid versus humid climates. This study suggests that pollen diversity indices have remarkable potential for quantitatively reconstructing paleoclimatic parameters.

1. Introduction

Biodiversity is threatened by global warming (Butchart et al., 2010; Cardinale et al., 2012), human activities (Zhang et al., 2024), and a mass extinction event (Ceballos et al., 2015; Raven and Wackernagel, 2020). Accordingly, there is an urgent need for heightened focus on forecasting and conserving biodiversity (Spicer et al., 2020; Senior et al., 2024). China, recognized as a global biodiversity hotspot (Zhang and Gilbert, 2015), houses the richest biodiversity in the Northern Hemisphere. However, biodiversity in the region is undergoing a severe decline (Qin and Zhao, 2017). Specifically, plant diversity has become a priority, as up to 10% of higher plant species have been designated as endangered (Qin et al., 2017). One approach to understanding how climate change and other factors may affect plant diversity is to elucidate the evolutionary patterns of plant diversity from past geological epochs. Identifying the factors that control these patterns can offer a historical perspective that is crucial for modern biodiversity conservation efforts; this is also essential for predicting future biodiversity trends and providing a scientific basis and guidance for

initiatives to create a sustainable and habitable Earth (Willis et al., 2010).

Previous studies have examined the evolution of paleobotanical diversity using plant fossils (Huang et al., 2016; Deng et al., 2019, 2020; Li et al., 2021; He et al., 2022; Zhou et al., 2023). However, the utility of plant fossils is limited by their specific preservation sites (Spicer and Wolfe, 1987), making it challenging to form a comprehensive understanding of the evolutionary history of plant diversity. Palynological indicators can effectively complement the deficiencies of plant fossils. Pollen grains offer the advantages of high productivity, easy preservation, and continuous deposition (Lu et al., 2011; Xu et al., 2014), which collectively allow for a detailed reconstruction of plant diversity characteristics and their dynamic evolutionary history across different periods (Jaramillo et al., 2006; Xiao et al., 2008; Li, 2018). Consequently, palynological indicators have become a pivotal tool for understanding the evolution of plant diversity.

Early studies in the 1970s and 1980s used specific diversity measurement methods, such as the Simpson index (Cwynar, 1982; Morley, 1982) and Shannon−Wiener index (Moore, 1973; Kuttel, 1984), to discuss changes in modern palynological diversity. However, these studies did not establish a link to plant diversity. In recent years, research has increasingly focused on the relationship between pollen diversity and plant diversity. Furthermore, changes in modern vegetation and the evolution of plant diversity during the Quaternary have been examined using different palynological diversity indices, including sporopollen richness (Seppa, 1998; Veski et al., 2005; Berglund et al., 2008; Valsecchi et al., 2010), sporopollen dominance (Xiao et al., 2008; Li, 2018), and evenness of sporopollen (Odgaard, 2001; Weng et al., 2006; Peros and Gajewski, 2008).

However, reconstructing paleovegetation diversity with palynological diversity indices remains challenging. These challenges stem from interspecies differences in pollen production, dispersal, and preservation (Goring et al., 2013), as well as varying classification accuracies. To address these issues, researchers have primarily used pollen richness or specific diversity indices as measures of palynological diversity to study the relationship between modern flora and palynological diversity. Most of this research has been concentrated in Europe, with relatively few studies in China (Cui et al., 2023; Chi et al., 2024b), and no consensus has yet been reached. Some scholars posit a positive relationship between modern palynological diversity and plant diversity (Meltsov et al., 2011; Felde et al., 2016; Reitalu et al., 2019; Abraham et al., 2020; Connor et al., 2021; Pardoe, 2021; Papadopoulou et al., 2022; Senn et al., 2022), whereas others argue that the relationship remains unclear (Goring et al., 2013; Gosling et al., 2018). The main reason for this discrepancy may be that most current studies are conducted on a relatively local scale, where climate and vegetation conditions do not vary markedly (Meltsov et al., 2013; Matthias et al., 2015). In addition, the use of different diversity indices across studies produces inconsistent findings and makes comparison difficult.

One solution to these limitations is to examine palynological diversity across regions with natural geographical differentiation on a large spatial scale. By comparing the results of different indices and selecting effective indices, a scientific basis can be provided for inferring the evolution of plant diversity using palynological data. In this study, we used a modern pollen database of China (Chen et al., 2021) to compare the accuracy of plant diversity reconstructions using five different palynological diversity indices over a large spatial scale. Specifically, we compared our calculations of each palynological index to the distribution of angiosperms in China (Lu et al., 2023) and identified which climatic parameters are correlated with these indices.

2. Materials and methods

Pollen data were extracted from a modern dataset of pollen in China (Chen et al., 2021; Fig. 1a). The data were preliminarily processed, which involved the removal of duplicates and low-quality samples, calibration of geographical coordinates, and standardization of pollen content, pollen taxon names, and data formats. Following the classification standards of the iPlant Flora platform from the Plant Science Data Center of the Chinese Academy of Sciences (https://www.plantplus.cn/cn; access on 21 March, 2024), the 772 pollen taxa in the dataset were categorized into angiosperms and gymnosperms.
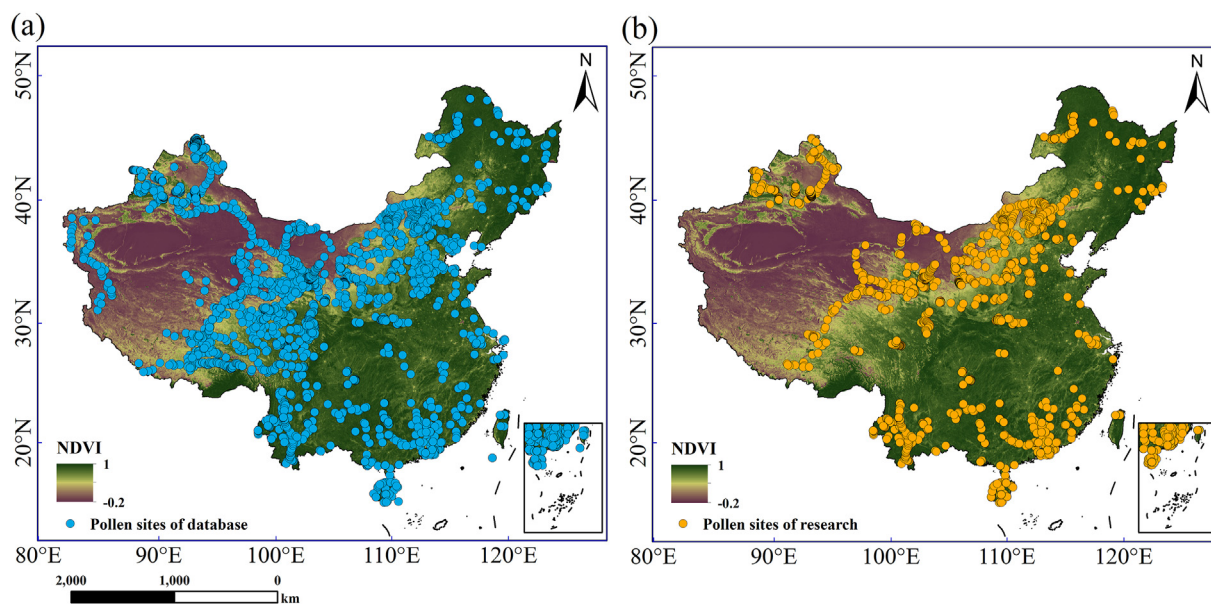

Fig. 1. Distribution maps of modern pollen samples. (a) Distribution of sample points of modern pollen in China (Chen et al., 2021). (b) Distribution map of pollen data samples used herein. NDVI, normalized difference vegetation index.

The plant diversity spatial distribution results used here for comparison were derived from a reconstruction of plant diversity spatial distribution using comprehensive richness and phylogenetic diversity indices as diversity indicators (Lu et al., 2023). Because only the diversity distribution of angiosperms is available, this study focuses solely on diversity analysis of angiosperm pollen in the dataset. The main taxa include *Artemisia*, Amaranthaceae, Asteraceae, *Betula*, Brassicaceae, *Carya*, *Carpinus*, *Corylus*, Cyperaceae, Fabaceae, *Juglans*, *Lonicera*, Leguminosae, *Melia*, Oleaceae, Poaceae, *Populus*, *Quercus*, Rosaceae, Ranunculaceae, *Ruta*, *Salix*, *Tilia*, *Tamarix*, *Ulmus*, and *Nitraria* (Chen et al., 2021).

The data source for the normalized difference vegetation index (NDVI) was the MOD13A3 dataset from the National Aeronautics and Space Administration (NASA), covering the period from February 2000 to December 2022 (https://ladsweb.modaps.eosdis.nasa.gov/) (Fig. 1). This dataset was used to generate monthly average NDVI data for the growing season (April–October) using the maximum value composite method.

2.1. Pollen data quality control

The modern pollen dataset of China integrates modern pollen samples from various datasets collected and analyzed by researchers for diverse purposes. Therefore, data quality control is indispensable. The purpose of pollen data quality control is to remove irrelevant pollen samples based on the objectives of this study, thereby reducing the possibility of data errors. For the samples in the dataset, we excluded several types of sample data based on their sources. The exclusion basis and steps were as follows.

1) Dating of pollen samples: we excluded samples from geological historical periods and high-resolution samples from stratigraphic columns. These stratigraphic samples span considerable periods of time and are primarily used to study vegetation succession, climate change, or the impact of climate change on vegetation since the Holocene or Last Glacial Maximum. The climate and vegetation conditions associated with these samples are markedly different from present-day conditions.
2) Study area and surrounding vegetation types: some samples in areas with intense human activity were removed, such as those associated with archeological sites and farmland. Such samples are mainly used to study the interaction between palynological assemblages, vegetation change, and human activity; hence, the results might not objectively reflect regional plant diversity.
3) Sampling source of palynological samples: non-topsoil pollen data were filtered. For example, samples from the surface sediments of lakes may be influenced by pollen carried by inflowing water (Wu et al., 2013), thereby affecting the reconstruction of local plant diversity.
4) Duplicate records: duplicate records were excluded to ensure that only one sample data point from each sampling site was used.

Through this screening process, we ensured that the data were reliable, effective, and of high quality; ultimately, 2245 topsoil pollen sample points were retained for this study (Fig. 1b; Appendix A).

2.2. Diversity indices and their calculation

Palynological diversity studies typically classify palynological diversity into richness, dominance, and evenness (Meltsov et al., 2011; Matthias et al., 2015). Currently, a number of common diversity indices are used in the quantitative expression of

palynological assemblages; these are outlined below (Eqs. (1)–(4)). The number of palynological species (S) represents the palynological richness, indicative of the number of pollen types in a sample (Rull, 1987); the Shannon−Wiener index (H) is an informative measure of palynological diversity (uncertainty) (Shannon, 1948), which is closely related to the number of palynological species (Eq. (1-1)). A higher number of palynological types in the sample results in higher uncertainty and indicates higher palynological diversity. The Simpson diversity index (D) measures the probability of palynological diversity (Simpson, 1949; Greenberg, 1956), describing the probability that two consecutive pollen grains from a bulk sample belong to the same species. A more uniform distribution of palynological types results in a higher likelihood of sampling the same species, indicating higher diversity; the value of this index ranges between 0 and 1 (Eq. (2)). The Berger−Parker index (d) is a measure of palynological dominance (Berger and Parker, 1970), with its equation describing the inverse of the relative abundance of the dominant palynological species (Eq. (3)). A higher index value indicates lower dominance of the dominant species, reflecting higher pollen diversity. The Hill index (D_q) is a measure of palynological diversity (Hill, 1973); its equation is expressed as the sum of all terms of the q-th power of pollen relative abundance (Pi) after the inverse transformation of the $1 - q$ exponent (Eq. (4-1)), q is a parameter that can be adjusted, and this parameter is generally an integer between 0 and 5. When $q = 0$, the Hill result (N0) and S are equal; when $q = 1$, the Hill result (N1) is similar to H; when $q = 2$, the Hill result (N2) is the reciprocal of $1 - D$, and when $q = 5$, the weight of the dominant species reaches its maximum and approaches the reciprocal of the abundance of the dominant species. This index simultaneously considers the palynological richness and evenness, and allows for different weighting of the two aspects by adjusting the parameter q. This is also referred to as the q-order diversity number, where an increase in q decreases the proportion of richness while increasing the proportion of evenness. To distinguish D_q results from those of S and H, we here adopted a Hill index with the parameter $q = 2$ (D_r; Eq. (4-2)). A higher number of sporopollen types and more uniform distribution of relative abundance result in a greater D_r value, indicating a higher diversity of sporopollen.

Current studies on palynology-plant diversity typically select specific diversity indices for investigation (Matthias et al., 2015; Felde et al., 2016; Papadopoulou et al., 2022; Liao et al., 2024), but the performances of many palynology-plant diversity indices in terms of plant diversity have not been measured. In this study, we calculated five diversity indices for pollen assemblages having more than one pollen type at each sample site in the dataset. This approach facilitates the selection of pollen diversity indices that are more representative of plant diversity by comparing the results of each index. All calculations were performed using Python 3.8, primarily utilizing the scientific computing library and associated tools, and using normalization to facilitate comparison with existing normalized plant diversity data. The equations for the calculations of the relevant indices are provided below:

$$H = -\sum_{i=1}^{S} P_i \log(P_i) \tag{1-1}$$

$$H = -\sum_{i=1}^{S} P_i \ln(P_i) \tag{1-2}$$

$$D = 1 - \sum_{i=1}^{S} P_i{}^2 \tag{2}$$

$$d = 1/P_{imax} \tag{3}$$

$$D_q = \sum_{i=1}^{S} \left(P_i{}^q\right)^{1/(1-q)} \tag{4-1}$$

$$D_r = 1 \bigg/ \sum_{i=1}^{S} P_i^2 \tag{4-2}$$

In these equations, S is the sum of palynological groups (number of family species) contained in each sample and P_i is the relative abundance of the i-th palynological group. The H index calculation (Eq. (1-1)) allows for the choice of the base e, 2, or 10. However, the H index value is usually < 4.5 (Magurran, 1988). By comparing the calculation results of different bases, e was ultimately selected as the base for calculation herein (Eqs. (1) and (2)).

2.3. Numerical methods of diversity reconstruction

To reconstruct the distribution pattern of angiosperm diversity using different diversity indices, we obtained the spatial pattern of angiosperm spore diversity in China. This was achieved by assigning the diversity data of the nearest pixel to each pollen sample point through Kriging interpolation based on the results of the spore diversity index (Krige, 1951). The reconstruction results of different indices were then compared with the current spatial distribution pattern of angiosperm diversity in China (Lu et al., 2023).

Evaluating image similarity facilitates the comparison of reconstruction results from various metrics with the spatial patterns of plant diversity, allowing for the identification of the most effective metrics. Common image similarity assessment methods include mean squared error, peak signal-to-noise ratio, and the structural similarity index measure (SSIM) (Samajdar and Quraishi, 2015). Of these, the SSIM is particularly advantageous because it captures structural changes and details in images, aligning more closely with human visual perception through its consideration of luminance, contrast, and structure when evaluating image similarity; this makes it a widely used metric for evaluating the similarity between two images (Wang et al., 2004). Image comparison was primarily conducted using the scikit-image library in Python 3.8, coupled with the SSIM correlation formula (Van der Walt et al., 2014). The SSIM has a range from 0 to 1, with values closer to 1 indicating more remarkable similarity between two images. To the best of our knowledge, this study is the first to employ SSIM to investigate pollen indices and reconstruct plant diversity. The related equations used in this process are detailed below (Eqs. 5–8):

Luminance similarity index:

$$l(x,y) = \left(2\mu_x\mu_y + C_1\right) \bigg/ \left(\mu_x^2 + \mu_y^2 + C_1\right) \tag{5}$$

Contrast similarity index:

$$c(x,y) = \left(2\sigma_x\sigma_y + C_2\right) \bigg/ \left(\sigma_x^2 + \sigma_y^2 + C_2\right) \tag{6}$$

Structure similarity index:

$$s(x,y) = \left(\sigma_{xy} + C_3\right) / \left(\sigma_x\sigma_y + C_3\right) \tag{7}$$

The final expression of the SSIM (Eq. (8)) can be obtained by multiplying the luminance similarity index (Eq. (5)), contrast similarity index (Eq. (6)), and structure similarity index (Eq. (7)):

$$SSIM(x,y) = \left(2\mu_x\mu_y + C_1\right)\left(2\sigma_{xy} + C_2\right) \bigg/ \left(\mu_x^2 + \mu_y^2 + C_1\right)\left(\sigma_x^2 + \sigma_y^2 + C_2\right) \tag{8}$$

where, $\mu_x = (1/N)\sum_{i=1}^{N} x_i$ is the mean value of pixels in image 1; $\mu_y = (1/N)\sum_{i=1}^{N} y_i$ is the mean value of pixels in image 2; $\sigma_x = ((1/N-1)\sum_{i=1}^{N}(x_i - \mu_x)^2)^{(1/2)}$ is the standard deviation of pixels for image 1; $\sigma_y = ((1/N-1)\sum_{i=1}^{N}(y_i - \mu_y)^2)^{(1/2)}$ is the standard deviation of pixels for image 2; and $\sigma_{xy} = (1/N-1)\sum_{i=1}^{N}(x_i - \mu_x)(y_i - \mu_y)$ is the pixel covariance of the two images. Small constants C_1, C_2, and C_3 are also introduced into the equation to avoid an unsolvable equation caused by a zero denominator.

2.4. Climate parameter acquisition

The modern climate data utilized in this study were based on observations from meteorological stations between 1980 and 2000. Using Python 3.8, we processed annual data from 518 meteorological stations across China, sourced from the National Center for Environmental Information (NCEI) (https://www.ncei.noaa.gov/data/global-summary-of-the-day/). This process included climate data extraction, station screening, parameter calculation, and data integration. Climate data for the pixel closest to each pollen sample site were assigned to the corresponding sample site using Kriging interpolation in Arcmap 10.8 (Krige, 1951). Four climatic parameters were extracted for each pollen sample site, including mean annual precipitation (P_{ann}), mean annual air temperature (T_{ann}), mean temperature of the coldest month (T_1, January), and mean temperature of the hottest month (T_7, July). The most representative plant diversity index was selected to explore the relationship between palynological diversity and these climatic variables based on the results of similarity measurement.

2.5. Numerical analysis of climatic factors

To explore the influence of climate on sporopollen diversity, Pearson correlation coefficients were employed to characterize the degree of linear correlation between sporopollen diversity and different climatic parameters. Before numerical analysis, we tested the collinearity between the climate and diversity data using a thermal correlation map to ensure that there was no over-fitting phenomenon. The size and significance of the correlation coefficients were used to assess the strength and relevance of the correlations. The correlation analysis was conducted using Python 3.8, primarily the Pandas and Matplotlib libraries. Building on these results, we explored the quantitative relationship between sporopollen diversity and climatic parameters in China. Dominant climatic factors influencing sporopollen diversity were identified based on the correlation results. The spatial contours of these factors were plotted using Arcmap 10.8 software, smoothed using the peak function, and then superimposed on the spatial pattern of sporopollen diversity. This approach allowed us to investigate the climatic variability in sporopollen diversity across a large spatial scale.

3. Results

3.1. Values of palynological diversity

Sporopollen diversity values were calculated according to the equations of different diversity indices. There were significant differences in the ranges of values among the various indices (Table 1). The distribution of results was more centralized for index D, while the ranges of values for the other indices were more disparate. The number of palynological species (S) ranged from 1 to 66, with a median of 11; index d varied from 1 to 15.33, with a median of 2.13;

Table 1
Indices of sporopollen diversity (S, d, D, D_r and H) and their descriptive statistical characterization.

Type of index	Richness S	Dominance d	Diversity D	Diversity D_r	Diversity H
Range of variation	1−66	1−15.33	0−1	1−27.64	0−3.67
Median	11	2.13	0.7	3.28	1.53
Standard deviation	8.63	1.38	0.21	3.14	0.68

index D varied from 0 to 1, with a median of 0.7; index D_r ranged from 1 to 27.64, with a median of 3.28; and index H varied from 0 to 3.67, with a median of 1.53 (Fig. 2).

These results indicate that S, H, d, and D_r are more sensitive to changes in species diversity than is D (Fig. 2c), because the data distribution ranges of the former are more extensive than that of the latter. Specifically, the index most responsive to changes in species diversity is the H index. The statistical distributions of the results show that S, d, and D_r account for progressively smaller proportions of the total as their values increase. In contrast, the results for H are more consistent with a normal distribution (Fig. 2e).

3.2. Spatial patterns of plant diversity reconstructed by palynological diversity indices

The results of each pollen diversity index were normalized and assigned to each pollen sample site. The diversity index value of the pixel closest to each sample site was allocated to that point using Kriging interpolation, resulting in maps depicting the distribution patterns of angiosperm pollen diversity in China under different indices (Fig. 3). The data normalization process can eliminate effects caused by the varying distribution ranges of different indices. Each of the diversity index maps closely resembled the spatial pattern of angiosperm diversity in China (Fig. 3a), generally indicating that diversity decreases from the southeast to northwest. SSIM image similarity metrics confirmed a high degree of similarity between the results of each diversity index and the spatial pattern of angiosperm diversity in China (Table 2); among these, the spatial pattern of the H index displayed the highest similarity (0.9), followed by those of d (0.75) and D (0.7). The pattern of S (0.625), an indicator of the number of pollen species, was also comparable. In contrast, D_r (0.5) was poorly representative of plant diversity (Fig. 3d). Correlation analysis showed that each pollen diversity index was positively correlated with plant diversity, corroborating our SSIM findings (Fig. 4). The H index had the highest correlation with plant diversity ($r = 0.63$) (Fig. 4a), followed by d (0.62) (Fig. 4b), D (0.57) (Fig. 4c), S (0.51) (Fig. 4d), and D_r (0.48) (Fig. 4e). This demonstrates that H and d are the most representative indicators of plant diversity among the pollen diversity indices studied herein.

3.3. Palynological diversity and climate

3.3.1. Statistical results of climatic factor interpolation

According to our spatial interpolation of climatic factors (Fig. 5), P_{ann} of modern topsoil sporopollen sample sites selected in this study ranged from 90 to 1909 mm, with a median of 476 mm (Fig. 5a); T_{ann} ranged from −1.3 to 25.5 °C, with a median of 8.3 °C (Fig. 5b); the distribution of the mean temperature of the coldest month (T_1, January) ranged from −26.1 to 20.4 °C, with a median of −7.6 °C (Fig. 5c); and the distribution of the mean temperature of the hottest month (T_7, July) ranged from 10.2 to 29.2 °C, with a median of 23.1 °C (Fig. 5d). In terms of temperature and precipitation, the palynological sample sites selected for this study cover a sufficiently broad climatic gradient to guarantee accurate analysis of the relationship between sporophyte diversity (based on the H index) and climate at a large spatial scale.

3.3.2. Relationship between palynological diversity and climate

To determine the relationship between palynological diversity and climate, we used the diversity index H, which strongly correlates with plant diversity. We compared the interpolated results of various climatic factors with this index to obtain the Pearson correlation coefficient (r). There were positive correlations between pollen diversity index H and P_{ann}, T_{ann}, T_1, and T_7 (Fig. 6). Of these, T_1 exhibited the highest correlation ($r = 0.49$), closely followed by T_{ann} ($r = 0.46$), then P_{ann} ($r = 0.38$), and finally T_7 ($r = 0.21$).

Annual precipitation of 400 mm is typically used as the demarcation line between humid-semi-humid and arid-semi-arid regions in China (Sun and Wang, 2005). This line, when plotted on a map, also aligns with the leading edge of the influence of the Asian summer monsoon. Here, we generated contour maps of P_{ann} (Fig. 7a) and T_1 (Fig. 8a) based on meteorological data and then superimposed the normalized results of the plant diversity index H (NH) on their respective distribution patterns (Figs. 7 and 8). The 400 mm precipitation line approximately coincided with the cutoff line where NH = 0.4 (Fig. 7b), except in northeastern regions; this NH = 0.4 line also approximately aligned with the contour line representing $T_1 = -6$ °C (Fig. 8b).

4. Discussion

4.1. Accuracy of palynological diversity indices in representing plant diversity

Calculating the spatial distribution of plant diversity is a particularly burdensome task. Previous studies that calculated the spatial distribution of angiosperms using diversity indices provide a valuable reference for our calculations of angiosperm diversity based on modern sporopollen data (Lu et al., 2023). In our study, we evaluated the advantages and limitations of five distinct diversity indices for pollen diversity. Specifically, each sporopollen diversity index was calculated. We then compared the spatial pattern of
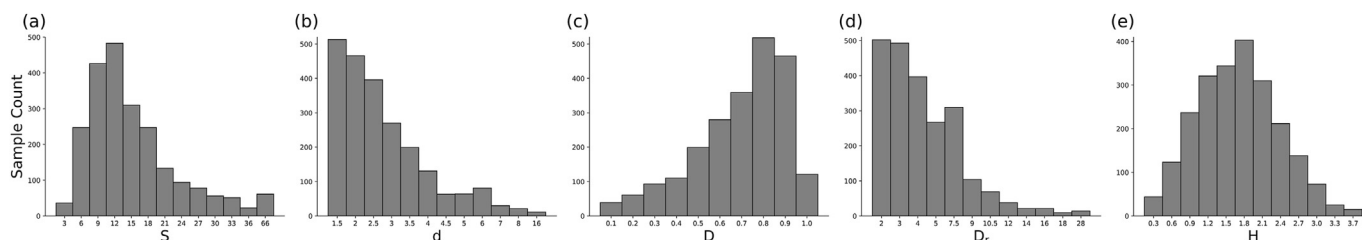

Fig. 2. Statistical ranges of indicators for angiosperm sporopollen diversity. (a) The number of palynological species, S; (b) Berger−Parker index, d; (c) Simpson diversity index, D, (d) Hill index, Dr; and (e) the Shannon−Wiener index, H.
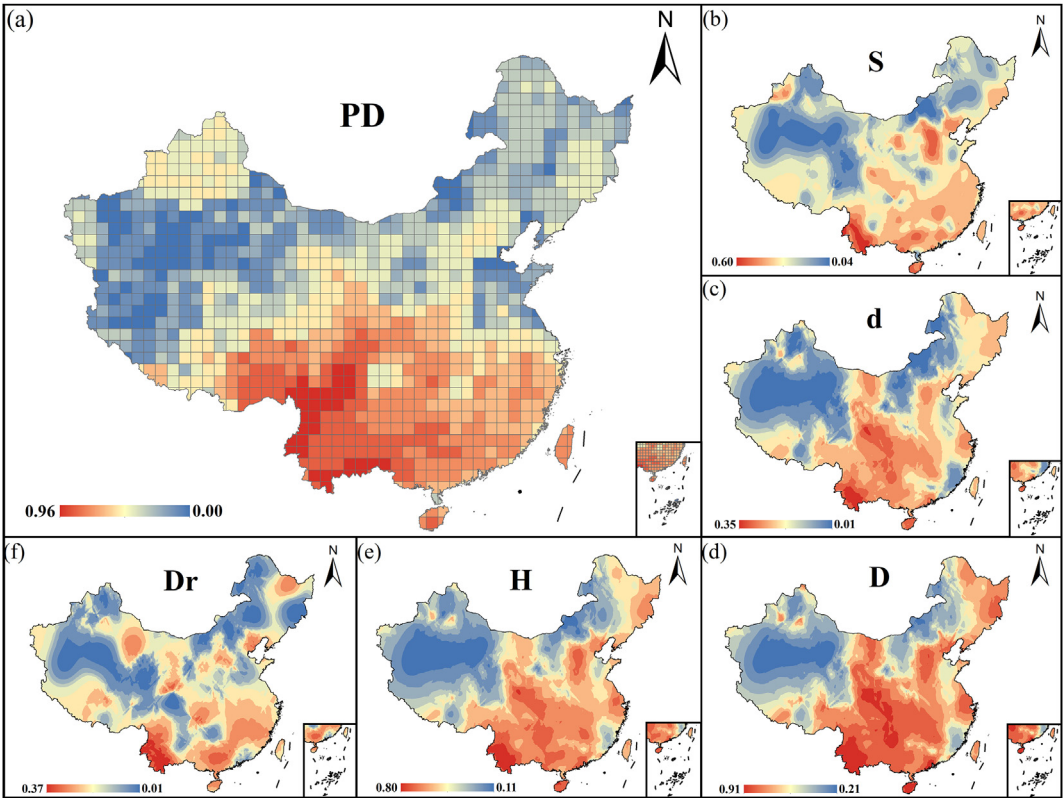
Fig. 3. Maps of spatial patterns of angiosperm diversity (PD (a), adapted from Lu et al. (2018) versus palynological diversity indices S (b), d (c), D_r (d), H (e), D (f).

Table 2
Calculated structural similarity index measure (SSIM) between palynological diversity and angiosperm diversity images.

Diversity indicators	S	d	D	D_r	H
SSIM	0.625	0.75	0.70	0.5	0.9

angiosperm pollen diversity from the normalized results with the distribution pattern of angiosperm diversity in China (Lu et al., 2023).

We found that the most index most representative of plant diversity is the Shannon−Wiener index (Table 2). The Shannon−Wiener index may have performed best because the sample sites selected in this study encompass a wide distribution range, large total sample size, and because the Shannon−Wiener index is better than other indices at distinguishing differences between samples. This has been confirmed in a study of insect diversity in which nine sites were compared using different diversity indices (Taylor, 1978). Similarly, a previous study based on pollen data from German lakes found that the Shannon−Wiener index outperformed other indices in determining the relationship between pollen and plant diversity (Matthias et al., 2015).

The next best indices were Berger−Parker index and the Simpson diversity index (Table 2). Although the Berger−Parker index is relatively rare in studies of palynological diversity, the results in this study are notable in their quality; this is probably because the Berger−Parker index only considers the dominant species in a community, making it highly sensitive to changes in species diversity and thus a good representation of plant diversity. The large scale of this study area and the extensive, comprehensive

selection of sample sites also contribute to its effectiveness (Su et al., 2017). Simpson diversity index has been widely used in past palynological research (Xiao et al., 2008; Wu et al., 2019; Cui et al., 2023) but its results have been inconsistent. For example, Cui et al. (2023) used the Simpson diversity index to reflect plant diversity based on palynological data, but the correlation only reached 0.33 after data correction. Herein, the Simpson diversity index performed worse at determining plant diversity than did the Shannon−Wiener or Berger−Parker index (SSIM = 0.7, $r = 0.57*$), and the proportion characteristics of numerical results are opposite to those of other indices. It may be that compared with other indices, the Simpson diversity index is less sensitive to changes in plant diversity, resulting in its slightly poorer representation of plant diversity (Su et al., 2017), as confirmed in previous studies (i.e., Matthias et al., 2015). Additionally, the applicability of the Simpson diversity index may be affected by variations in the form of the equation used by different researchers; hence, any determination of its applicability needs to pay attention to the parameters reflected by the diversity index equation, highlighting the importance of understanding the specific aspects of diversity that each equation reflects.

The number of palynological species (S) has long been regarded as representative of palynological richness. Some researchers have further refined this approach, suggesting that the S value after rarefaction treatment may better reflect plant diversity (Simberloff, 1972; Birks and Line, 1992; Li and Zhao, 2018; Cui et al., 2023). Rarefaction entails randomly selecting a certain number of sporopollen individuals from a bulk sample, counting the number of sporopollen types represented in this subset, and accumulating these counts until a set standard is reached. This process can avoid
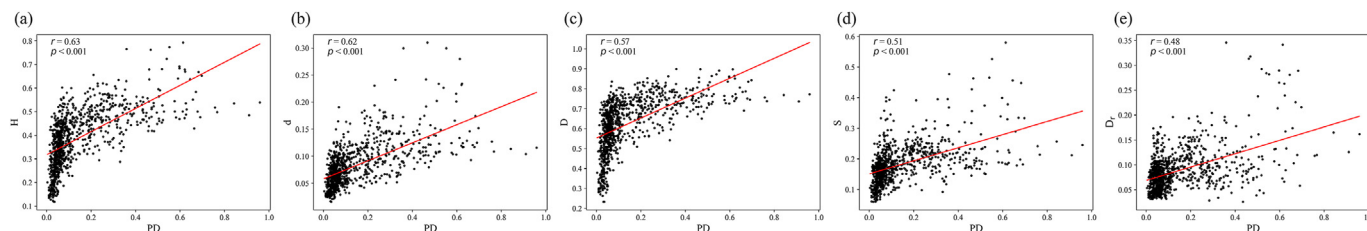
Fig. 4. Correlation analysis of plant diversity (PD) and palynological diversity indices H (a), d (b), D (c), S (d), D_r (e).
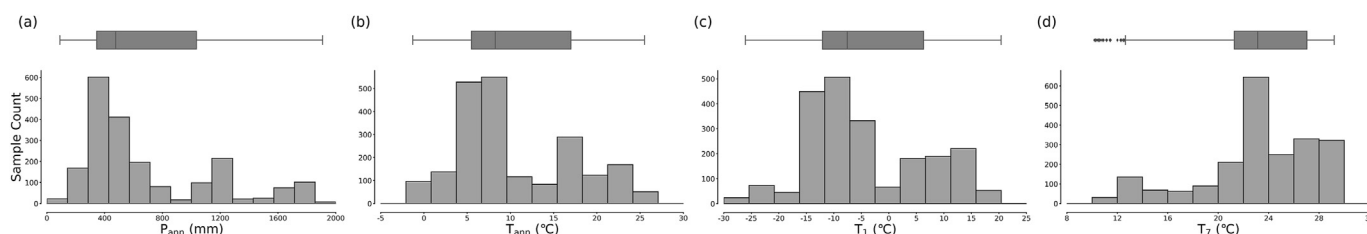

Fig. 5. Climatic conditions at modern palynological sites. (a) Annual precipitation, P_{ann}; (b) annual temperature, T_{ann}; (c) mean temperature of the coldest month, T_1; (d) mean temperature of the hottest month, T_7. In each of the plots, a histogram of the distribution of the climate factor data is shown at the bottom, and the corresponding box-and-line plot is shown at the top. Boxplots represent the first through third quartile ranges of the data distribution, the vertical line in the box represents the median of the data, the short vertical line at the end of the horizontal line outside the box represents the minimum and maximum of the data, respectively, and the data points outside the box represent outliers.

errors caused by differences in the number of sporopollen grains across different samples; i.e., the diversity of different samples is compared under a unified standard to effectively evaluate palynological diversity. Jaramillo et al. (2006) used the S value after rarefaction to reconstruct plant diversity in the Neotropics during the Cenozoic, revealing that diversity fluctuations were closely related to global temperature changes. However, the rarefaction process requires original pollen data (i.e., the number of pollen grains) (Birks and Line, 1992); the database used herein only contained percentage data, not original statistics, so the rarefaction process could not be applied in this study. Consequently, the representativeness of S value in terms of plant diversity may have been affected, with the correlation only reaching 0.625. This index may perform better after rarefaction.

Our analysis indicates that the index that least represents plant diversity is the Hill index (D_r) (SSIM = 0.5, r = 0.48). The Hill index is commonly applied to the study of palynological diversity by adjusting for different past parameters (Felde et al., 2016; Gosling et al., 2018; Chi et al., 2024b), because this index can comprehensively measure the dominance and evenness of plants through adjusting its equation. For example, S (N0), H (N1), and D_r (N2) are derived using the adjustable characteristics of the Hill equation (Wang et al., 2022). This approach essentially utilizes S and H as diversity research indicators, indicating that the Hill index cannot replace S, H, or other indices. To circumvent this issue, we only used the Hill index, D_r, with a parameter of q = 2. However, the results exhibited poor representativeness. The accuracy of biodiversity reflected by palynological data may be improved by using a combination of the number of palynological species and the Shannon−Wiener index after rarefaction, or selectively adding correction methods according to parameter differences when using the Hill index. Palynological productivity and spread rate may also affect the reconstruction of plant diversity (Jaramillo et al., 2006; Giesecke et al., 2014). Considering these factors, some researchers have used the REVEALS model or R value to correct pollen data. This may be an effective way to improve the representativeness of palynological diversity in relation to plant diversity (Cui et al., 2023; Xia and Ni, 2024).

4.2. Factors influencing the spatial patterns of palynological diversity

Correlation analysis indicated that of the climate factors analyzed palynological diversity is most affected by the mean temperature of the coldest month and annual precipitation. The correlation coefficient between the mean temperature of the coldest month and the Shannon−Wiener index of palynological diversity was 0.49 without using a calibration model, and that between annual precipitation and palynological diversity was 0.38. In contrast, annual temperature and the mean temperature of the hottest month had relatively little influence on palynological diversity. These combined data indicate that the main climatic factor that determines the level of palynological diversity amongst angiosperms is the degree of coldness during winter.

Our findings on the impact of the temperature of the coldest month of the year are consistent with previous studies (Wang et al., 2011; Qian, 2013). For example, redundancy analysis in the Hengduan Mountains also found that the most critical factor in determining palynological assemblages in the region was mean temperature of the coldest month (Chi et al., 2024a). Studies conducted on the Tibetan Plateau, southwest Yunnan, and other regions also suggest that the distribution of palynological assemblages is markedly influenced by the mean temperature of the coldest month (Wang et al., 2022; Xiao et al., 2023). The primary reason that palynological assemblages are negatively impacted by the coldest month of the year is that low temperatures stymie the growth and development of plants (Winfield et al., 2010; Zhou et al., 2018), limiting the distribution of plants and vegetation types (Woodward and Williams, 1987). Studies on plant diversity also indicate that the mean temperature of the coldest month substantially impact plant diversity (Wang et al., 2011; Song et al., 2024). Furthermore, the mean temperature of the coldest month has been shown to affect the spatial distribution patterns of woody plant diversity in China (Wang et al., 2011).

Other research also suggests that palynological assemblages are greatly affected by annual precipitation (Lu et al., 2011; Qian, 2013; Cao et al., 2014, 2021; Chi et al., 2024b). Specifically, in the Medog
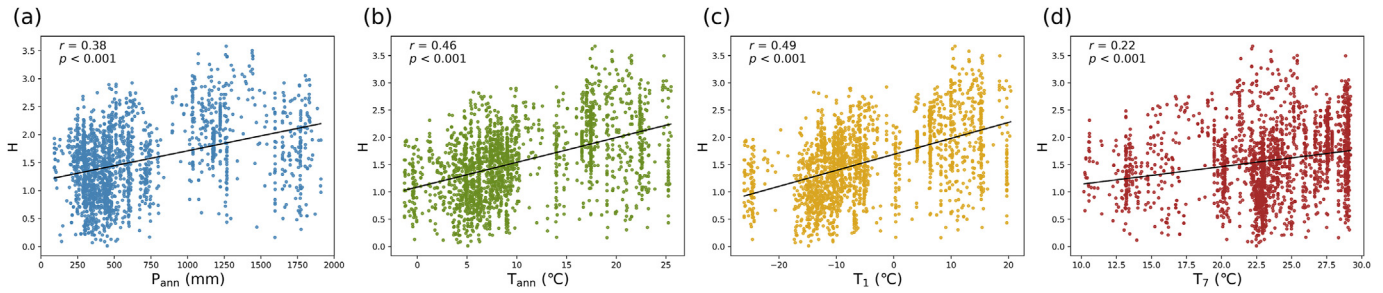
Fig. 6. Linear plots of palynological diversity (H index) versus climatic elements P_{ann} (a), T_{ann} (b), T_1 (c), T_7 (d).
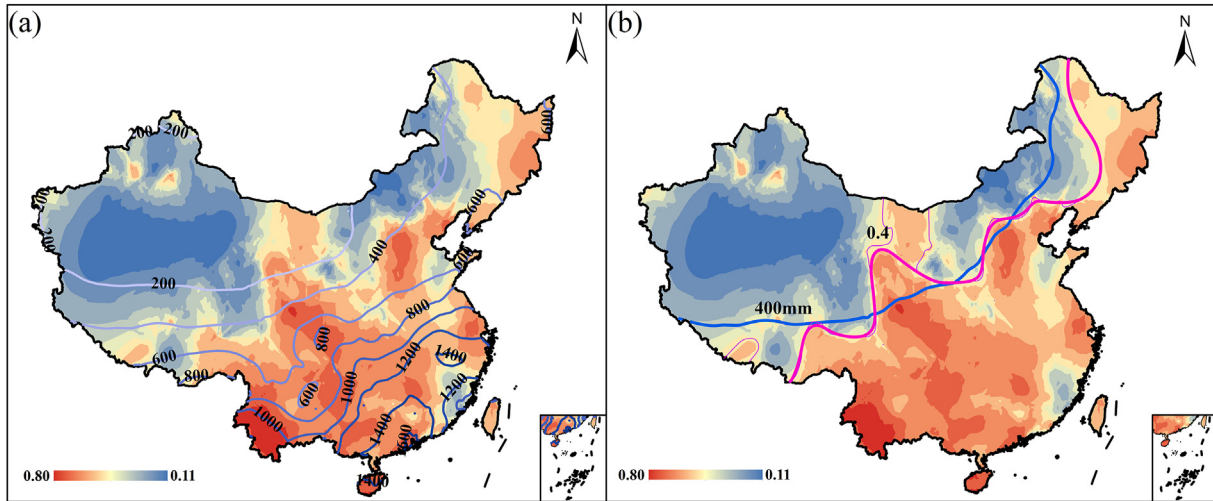

Fig. 7. Spatial pattern of palynological diversity in relation to mean annual precipitation (P_{ann}) contours. (a) Contour overlay of P_{ann} on palynological diversity. (b) Map highlighting the P_{ann} = 400 mm contour line (thick blue), normalized H index (NH) = 0.4 contour line (thin purple) and its approximate line (thick pink).
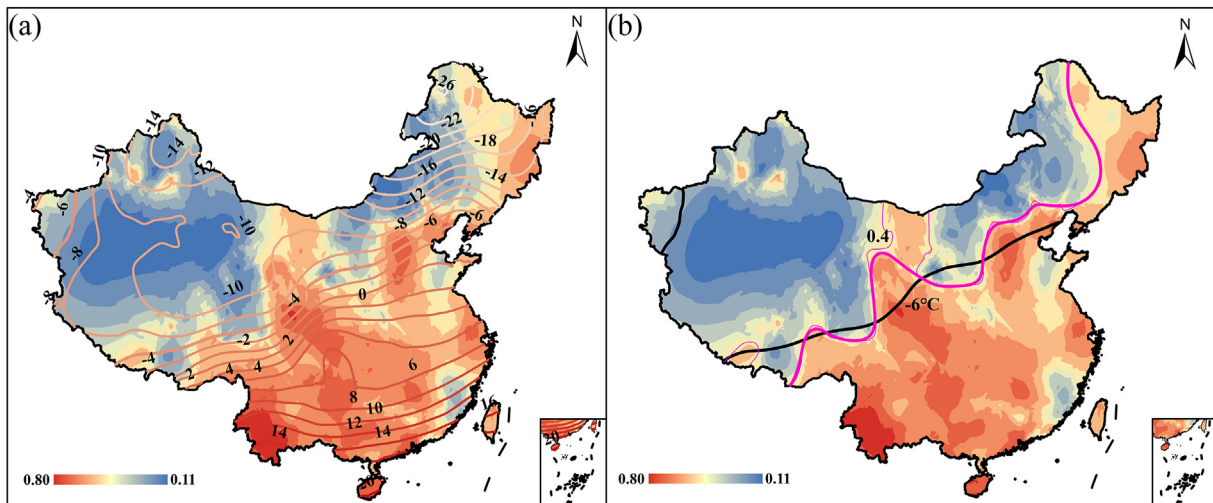

Fig. 8. Spatial pattern of palynological diversity in relation to mean temperature of the coldest month (T_1) contours. (a) Overlay of T_1 contours on palynological diversity. (b) Map highlighting the T_1 = −6 °C contour line (thick black), normalized H index (NH) = 0.4 contour line (thin purple) and its approximate line (thick pink).

Mountains of the Tibetan Plateau, *Cyclobalanopsis* and *Abies* exhibit a clear preference for a humid environment (Chi et al., 2024b). In Southeast Asia, a sporopollen study of forest vegetation identified pollen indicative of high precipitation, such as *Nepenthes* and *Adhatoda* (Basumatary et al., 2014), and found that the proportion of woody plant pollen types was relatively high. Consequently,

many researchers infer that annual precipitation is the dominant climatic factor controlling palynological assemblages. Additionally, some studies have suggested that mean temperature of the hottest month also greatly affects palynological assemblages (Shen et al., 2006; Wei et al., 2011; Zhang et al., 2020). For example, redundancy analysis found that sporopollen assemblages on the southern

slopes of the Himalayas were most affected by mean temperature of the hottest month (Zhang et al., 2020). However, their study was confined to a high-elevation region with a limited climatic gradient, rendering the findings less representative.

Differences in the dominant climatic factors affecting palynological assemblages may be related to the spatial range of sample site distribution and the specific palynological assemblages studied. Research in which there is a broader distribution of sample sites generally supports the notion that mean temperature of the coldest month is the most important climatic factor (Chi et al., 2024a). Additionally, sensitivities to climate change differ between herbaceous and woody plants (Lu et al., 2018; Song et al., 2024). Thus, the proportions of such species in a palynological assemblage may also have an impact. Because there are currently few studies on the influence of climate on palynological diversity at a large spatial scale, our study provides a pioneering reference.

In China, annual precipitation and angiosperm pollen diversity share a similar distribution pattern: high values in the southeast and low values in the northwest (Fig. 8a). The 400 mm precipitation threshold line marks the east-west differentiation between wet-sub-humid and drought-semi-arid regions in China (Sun and Wang, 2005). It also aligns with the east-west divergence line of the evolutionary history of angiosperms (Zhao et al., 2023) and the leading edge of the Asian monsoon influence (Wu et al., 2022). This line holds important geographical and ecological significance. In this study, the angiosperm pollen diversity based on the Shannon−Wiener index was compared with precipitation contour lines in China. We found that the 400 mm contour line effectively distinguishes levels of palynological diversity. Palynological diversity (i.e., NH value) southeast of this line was generally > 0.4. The large latitude difference and stronger monsoon influence in the southeast results in a higher and more complex pattern of palynological diversity. However, in the northwest, the pattern of angiosperm sporopollen diversity was relatively undifferentiated and concentrated at low diversity levels. Eastern China, located in the Asian monsoon zone, experiences synchronous rain and heat, which alters plant phenology and promotes plant growth and pollen production (Zhang and Steiner, 2022; Zu et al., 2024). Furthermore, stronger monsoon winds and a warmer, wetter climate leads to an increase in the number of trees (Basumatary et al., 2014; Zhao et al., 2020), which in turn leads to a higher sporopollen diversity in angiosperms. The east-west difference in angiosperm spore diversity is also consistent with the phylogenetic history of angiosperms. Eastern China serves as the evolutionary cradle of woody plants, whereas western China is the evolutionary cradle of herbaceous genera (Lu et al., 2018). Notably, within areas of generally high diversity in southeastern coastal China, there are a few areas with low palynological diversity. This discrepancy is related to the location of sample sites and palynological identification. These data are derived from the modern palynological database of East Asia, which ensures the reliability of data quality to some extent, however, the selection of sample sites may be biased, affecting the palynological diversity results. Moreover, when we analyzed these low-diversity sample sites, we found that these areas are mainly in subtropical evergreen broadleaf forests dominated by *Castanopsis fargesii* forest, but that different species in *C. fargesii* forests were mostly merged into a single *Castanopsis* taxon due to inaccurate identification. This may have reduced the number of sporopollen species in the samples, resulting in low diversity values in some southeastern coastal areas. Similarly, in a study on pollen-vegetation representativeness based on R values, it was also found that the R value of *Castanopsis* was very low (only 0.03; Xia and Ni, 2024), indicating that the identification of this genus may be underestimated compared with the actual number of plants; hence, the low sporopollen diversity in some southeastern

coastal areas without numerical correction appears to be within a reasonable range.

When we compared the angiosperm pollen diversity obtained herein with contours of the mean temperature of the coldest month in China, we found that the normalized H index (NH) = 0.4 contour line also approximately coincided with the −6 °C contour for the mean temperature of the coldest month, except in northeastern China. Studies have shown that mean temperature of the coldest month has different effects on the palynology of different plant groups, with herbaceous plants being more affected than woody plants (Song et al., 2024). These findings suggest that the ratio of woody to herbaceous plants in the dataset may influence the effect of the mean temperature of the coldest month on palynological diversity. Previous paleoclimatic reconstructions using sporopollen analysis have primarily considered the effect of annual temperature on sporopollen assemblages, often overlooking the impact of the coldest month (Herzschuh et al., 2014; Opitz et al., 2015). The temperature of the coldest month is also overlooked in paleoclimatic reconstructions based on sporopollen diversity, indicating that sporopollen diversity correlates with temperature but including errors (Jaramillo et al., 2006). In a study that reconstructed paleo-vegetation, analyses based on sporopollen assemblages from 94 regions worldwide suggested that vegetation changes since the last glacial period have been primarily driven by winter temperatures, except in the tropics (Harrison and Goñi, 2010). A related study on southwest China also indicated that the development of evergreen and deciduous broadleaf forests and subalpine scrub in the region has been controlled by winter temperatures over the past 1.2 ka (Ni et al., 2019). Therefore, increased attention needs to be paid to the effect of winter temperature on vegetation and diversity in studies related to pollen diversity during historical periods.

5. Conclusions

In this study, we used a modern pollen database of China to compare the accuracy of plant diversity reconstructions using five different palynological diversity indices over a large spatial scale. Additionally, we explored the relationship between palynological diversity, as measured by the Shannon−Wiener index, and various climatic factors. We found that the Shannon−Wiener index and Berger−Parker index outperformed other indices in reconstructing plant diversity, demonstrating great potential for reconstructing the history of plant diversity. However, considering the influence of factors such as pollen yield and sedimentation rate, we cannot rule out better performance of the other indices when applying the correction method, especially the S index after the rarefaction. Thus, the other indices may also have great potential in reconstructing plant diversity history and need to be further tested. In addition, numerical analysis of palynological diversity (based on the H index) and climatic parameters revealed that plant diversity is significantly affected by mean temperature of the coldest month and annual precipitation, with both parameters showing positive correlations with plant diversity. Furthermore, a normalized value of 0.4 for the H index (NH = 0.4) can serve as an approximate threshold for determining the reconstruction of plant diversity under the influence of arid versus humid climates. Our study provides a modern approach for reconstructing the evolutionary history of paleovegetation diversity using palynological indices.

CRediT authorship contribution statement

Yuxuan Jiang: Writing − original draft, Software, Formal analysis. **Fuli Wu:** Writing − review & editing, Supervision, Funding acquisition. **Xiaomin Fang:** Writing − review & editing, Supervision, Methodology, Funding acquisition. **Haitao Wang:**

Visualization, Formal analysis. **Yulong Xie:** Data curation. **Cuirong Yu:** Investigation.

Declaration of competing interest

The authors declare that they have no known competing financial interests or personal relationships that could have appeared to influence the work reported in this paper.

Acknowledgements

Appendix A. Supplementary data

Supplementary data to this article can be found online at https://doi.org/10.1016/j.pld.2025.01.004.

References

Abraham, V., Roleček, J., Vild, O., et al., 2020. Spatial scaling of pollen-based alpha and beta diversity within forest and open landscapes of Central Europe. bioRxiv 2020—8. https://doi.org/10.1101/2020.08.18.255737.

Basumatary, S., Bera, S., Sangma, S., et al., 2014. Modern pollen deposition in relation tovegetation and climate of Balpakram valley, Meghalaya, northeast India: implications for Indo-Burma palaeoecological contexts. Quat. Int. 325, 30—40. https://doi.org/10.1016/j.quaint.2013.08.013.

Berger, W.H., Parker, F.L., 1970. Diversity of planktonic foraminifera in deep-sea sediments. Science 168, 1345—1347. https://doi.org/10.1126/science.168.3937.1345.

Berglund, B.E., Gaillard, M.-J., Björkman, L., et al., 2008. Long-term changes in floristic diversity in southern Sweden: palynological richness, vegetation dynamics and land-use. Veg. Hist. Archaeobot. 17, 573—583. https://doi.org/10.1007/s00334-007-0094-x.

Birks, H.J.B., Line, J.M., 1992. The use of rarefaction analysis for estimating palynological richness from Quaternary pollen-analytical data. Holocene 2, 1—10. https://doi.org/10.1177/095968369200200101.

Butchart, S.H., Walpole, M., Collen, B., et al., 2010. Global biodiversity: indicators of recent declines. Science 328, 1164—1168. https://doi.org/10.1126/science.1187512.

Cao, X.Y., Tian, F., Li, K., et al., 2021. Lake surface-sediment pollen dataset for the alpine meadow vegetation type from the eastern Tibetan Plateau and its potential in past climate reconstructions. Earth Syst. Sci. Data Discuss. 1—22. https://doi.org/10.5194/essd-13-3525-2021, 2021.

Cao, X.Y., Herzschuh, U., Telford, R.J., et al., 2014. A modern pollen—climate dataset from China and Mongolia: assessing its potential for climate reconstruction. Rev. Palaeobot. Palynol. 211, 87—96. https://doi.org/10.1016/j.revpalbo.2014.08.007.

Cardinale, B.J., Duffy, J.E., Gonzalez, A., et al., 2012. Biodiversity loss and its impact on humanity. Nature 486, 59—67. https://doi.org/10.1038/nature11148.

Ceballos, G., Ehrlich, P.R., Barnosky, A.D., et al., 2015. Accelerated modern human—induced species losses: entering the sixth mass extinction. Sci. Adv. 1, e1400253. https://doi.org/10.1126/sciadv.1400253.

Chen, H.Y., Xu, D.Y., Liao, M.N., et al., 2021. A modern pollen dataset of China. Chin. J. Plant Ecol. 45, 799. https://doi.org/10.17521/cjpe.2021.0024.

Chi, C.T., Xiao, X.Y., Jia, B.Y., 2024a. Modern vegetation-climate relationships for pollen assemblages across the mountainous regions of southwestern China: implications for palaeoenvironmental reconstruction. Palaeogeogr. Palaeoclimatol. Palaeoecol. 644, 112211. https://doi.org/10.1016/j.palaeo.2023.112211.

Chi, C.T., Xiao, X.Y., Wang, J.J., et al., 2024b. The vertical distribution of modern pollen in the southeastern edge of the Tibetan Plateau, China. Palynology 48, 2258941. https://doi.org/10.1080/01916122.2023.2258941.

Connor, S.E., van Leeuwen, J.F., van der Knaap, W.O., et al., 2021. Pollen and plant diversity relationships in a Mediterranean montane area. Veg. Hist. Archaeobot. 30, 583—594. https://doi.org/10.1007/s00334-020-00811-0.

Cui, Y.F., Qin, F., Zhao, Y., et al., 2023. Does palynological diversity reflect floristic diversity? A case study from Northeast China. Sci. China Earth Sci. 66, 2097—2108. https://doi.org/10.1007/s11430-022-1131-y.

Cwynar, L.C., 1982. A late-quaternary vegetation history from hanging lake, northern yukon: ecological archives m052-001. Ecol. Monogr. 52, 1—24. https://doi.org/10.2307/2937323.

Deng, T., Wu, F.X., Wang, S.Q., et al., 2019. Significant shift in the terrestrial ecosystem at the Paleogene/Neogene boundary in the Tibetan Plateau. Chin. Sci. Bull. 64, 2894—2906. https://doi.org/10.1360/TB-2019-0053.

Deng, W.Y.D., Su, T., Wappler, T., et al., 2020. Sharp changes in plant diversity and plant-herbivore interactions during the Eocene—Oligocene transition on the southeastern Qinghai-Tibetan Plateau. Global Planet. Change 194, 103293. https://doi.org/10.1016/j.gloplacha.2020.103293.

Felde, V.A., Peglar, S.M., Bjune, A.E., et al., 2016. Modern pollen—plant richness and diversity relationships exist along a vegetational gradient in southern Norway. Holocene 26, 163—175. https://doi.org/10.1177/0959683615596843.

Giesecke, T., Ammann, B., Brande, A., 2014. Palynological richness and evenness: insights from the taxa accumulation curve. Veg. Hist. Archaeobot. 23, 217—228. https://doi.org/10.1007/s00334-014-0435-5.

Goring, S., Lacourse, T., Pellatt, M.G., et al., 2013. Pollen assemblage richness does not reflect regional plant species richness: a cautionary tale. J. Ecol. 101, 1137—1145. https://doi.org/10.1111/1365-2745.12135.

Gosling, W.D., Julier, A.C., Adu-Bredu, S., et al., 2018. Pollen-vegetation richness and diversity relationships in the tropics. Veg. Hist. Archaeobot. 27, 411—418. https://doi.org/10.1007/s00334-017-0642-y.

Greenberg, J.H., 1956. The measurement of linguistic diversity. Language 32, 109—115. https://doi.org/10.2307/410659.

Harrison, S., Goñi, M.S., 2010. Global patterns of vegetation response to millennial-scale variability and rapid climate change during the last glacial period. Quat. Sci. Rev. 29, 2957—2980. https://doi.org/10.1016/j.quascirev.2010.07.016.

He, S.L., Ding, L., Xiong, Z.Y., et al., 2022. A distinctive Eocene Asian monsoon and modern biodiversity resulted from the rise of eastern Tibet. Sci. Bull. 67, 2245—2258. https://doi.org/10.1016/j.scib.2022.10.006.

Herzschuh, U., Borkowski, J., Schewe, J., et al., 2014. Moisture-advection feedback supports strong early-to-mid Holocene monsoon climate on the eastern Tibetan Plateau as inferred from a pollen-based reconstruction. Palaeogeogr. Palaeoclimatol. Palaeoecol. 402, 44—54. https://doi.org/10.1016/j.palaeo.2014.02.022.

Hill, M.O., 1973. Diversity and evenness: a unifying notation and its consequences. Ecology 54, 427—432. https://doi.org/10.2307/1934352.

Huang, Y.J., Jia, L.B., Wang, Q., et al., 2016. Cenozoic plant diversity of Yunnan: a review. Plant Divers. 38, 271—282. https://doi.org/10.1016/j.pld.2016.11.004.

Jaramillo, C., Rueda, M.J., Mora, G., 2006. Cenozoic plant diversity in the Neotropics. Science 311, 1893—1896. https://doi.org/10.1126/science.1121380.

Krige, D.G., 1951. A statistical approach to some basic mine valuation problems on the Witwatersrand. J. S. Afr. Inst. Min. Metall 52, 119—139.

Kuttel, M., 1984. Veränderung von Diversität und Evenness der Tundra, aufgezeichnet im Pollendiagramm des Vuolep Allakasjaure. Bot. Helv. 94, 279—283.

Li, Q., 2018. Spatial variability and long-term change in pollen diversity in Nam Co catchment (central Tibetan Plateau): implications for alpine vegetation restoration from a paleoecological perspective. Sci. China Earth Sci. 61, 270—284. https://doi.org/10.1007/s11430-017-9133-0.

Li, Q., Zhao, Y., 2018. Quantitative methods and progress of paleo-floristic diversity reconstruction based on pollen assemblages. Quat. Sci. 38, 821—829. https://doi.org/10.11928/j.issn.1001-7410.2018.04.02.

Li, S.F., Valdes, P.J., Farnsworth, A., et al., 2021. Orographic evolution of northern Tibet shaped vegetation and plant diversity in eastern Asia. Sci. Adv. 7, eabc7741. https://doi.org/10.1126/sciadv.abc7741.

Liao, M.L., Jin, Y.L., Li, K., et al., 2024. Modern pollen-plant diversity relationship in open landscapes of Tibetan Plateau. Palaeogeogr. Palaeoclimatol. Palaeoecol. 641, 112131. https://doi.org/10.1016/j.palaeo.2024.112131.

Lu, H.Y., Wu, N.Q., Liu, K.B., et al., 2011. Modern pollen distributions in Qinghai-Tibetan Plateau and the development of transfer functions for reconstructing Holocene environmental changes. Quat. Sci. Rev. 30, 947—966. https://doi.org/10.1016/j.quascirev.2011.01.008.

Lu, L.M., Zhao, L., Hu, H.H., et al., 2023. A comprehensive evaluation of flowering plant diversity and conservation priority for national park planning in China. Fundam. Res. 3, 939—950. https://doi.org/10.1016/j.fmre.2022.08.008.

Lu, L.M., Mao, L.F., Yang, T., et al., 2018. Evolutionary history of the angiosperm flora of China. Nature 554, 234—238. https://doi.org/10.1038/nature25485.

Magurran, A.E., 1988. Ecological Diversity and its Measurement. Princeton University Press, Princeton.

Matthias, I., Semmler, M.S.S., Giesecke, T., 2015. Pollen diversity captures landscape structure and diversity. J. Ecol. 103, 880—890. https://doi.org/10.1111/1365-2745.12404.

Meltsov, V., Poska, A., Odgaard, B.V., et al., 2011. Palynological richness and pollen sample evenness in relation to local floristic diversity in southern Estonia. Rev. Palaeobot. Palynol. 166, 344—351. https://doi.org/10.1016/j.revpalbo.2011.07.001.

Meltsov, V., Poska, A., Reitalu, T., et al., 2013. The role of landscape structure in determining palynological and floristic richness. Veg. Hist. Archaeobot. 22, 39—49. https://doi.org/10.1007/s00334-012-0358-y.

Moore, P.D., 1973. The influence of prehistoric cultures upon the initiation and spread of blanket bog in upland Wales. Nature 241, 350–353. https://doi.org/10.1038/241350a0.

Morley, R.J., 1982. A palaeoecological interpretation of a 10,000 year pollen record from Danau Padang, Central Sumatra, Indonesia. J. Biogeogr. 9, 151–190. https://doi.org/10.2307/2844699.

Ni, Z.Y., Jones, R., Zhang, E.N., et al., 2019. Contrasting effects of winter and summer climate on Holocene montane vegetation belts evolution in southeastern Qinghai-Tibetan Plateau, China. Palaeogeogr. Palaeoclimatol. Palaeoecol. 533, 109232. https://doi.org/10.1016/j.palaeo.2019.06.005.

Odgaard, B.V., 2001. Palaeoecological perspectives on pattern and process in plant diversity and distribution adjustments: a comment on recent developments. Divers. Distrib. 7, 197–201. https://doi.org/10.1111/j.1472-4642.2001.00110.x.

Opitz, S., Zhang, C.J., Herzschuh, U., et al., 2015. Climate variability on the southeastern Tibetan Plateau since the Lateglacial based on a multiproxy approach from Lake Naleng—comparing pollen and non-pollen signals. Quat. Sci. Rev. 115, 112–122. https://doi.org/10.1016/j.quascirev.2015.03.011.

Papadopoulou, M., Tsiripidis, I., Panajiotidis, S., et al., 2022. Testing the potential of pollen assemblages to capture composition, diversity and ecological gradients of surrounding vegetation in two biogeographical regions of southeastern Europe. Veg. Hist. Archaeobot. 31, 1–15. https://doi.org/10.1007/s00334-021-00831-4.

Pardoe, H.S., 2021. Identifying floristic diversity from the pollen record in open environments; considerations and limitations. Palaeogeogr. Palaeoclimatol. Palaeoecol. 578, 110560. https://doi.org/10.1016/j.palaeo.2021.110560.

Peros, M.C., Gajewski, K., 2008. Testing the reliability of pollen-based diversity estimates. J. Paleolimnol. 40, 357–368. https://doi.org/10.1007/s10933-007-9166-2.

Qian, H., 2013. Environmental determinants of woody plant diversity at a regional scale in China. PLoS One 8, e75832. https://doi.org/10.1371/journal.pone.0075832.

Qin, H.N., Zhao, L.N., 2017. Evaluating the threat status of higher plants in China. Biodivers. Sci. 25, 689. https://doi.org/10.17520/biods.2017007.

Qin, H.N., Zhao, L.N., Yu, S.X., et al., 2017. Evaluating the endangerment status of China's angiosperms through the red list assessment. Biodivers. Sci. 25, 745–757. https://doi.org/10.17520/biods.2017156.

Raven, P., Wackernagel, M., 2020. Maintaining biodiversity will define our long-term success. Plant Divers. 42, 211–220. https://doi.org/10.1016/j.pld.2020.06.002.

Reitalu, T., Bjune, A.E., Blaus, A., et al., 2019. Patterns of modern pollen and plant richness across northern Europe. J. Ecol. 107, 1662–1677. https://doi.org/10.1111/1365-2745.13134.

Rull, V., 1987. Note on pollen counting in palaeoecology. Pollen Spores 29, 471–477.

Samajdar, T., Quraishi, M.I., 2015. Analysis and evaluation of image quality metrics. In: Information Systems Design and Intelligent Applications: Proceedings of Second International Conference INDIA, vol. 2, pp. 369–378. https://doi.org/10.1007/978-81-322-2247-7-38, 2015.

Senior, R.A., Bagwyn, R., Leng, D., et al., 2024. Global shortfalls in documented actions to conserve biodiversity. Nature 630, 387–391. https://doi.org/10.1038/s41586-024-07498-7.

Senn, C., Tinner, W., Felde, V.A., et al., 2022. Modern pollen-vegetation-plant diversity relationships across large environmental gradients in northern Greece. Holocene 32, 159–173. https://doi.org/10.1177/09596836221060494.

Seppä, H., 1998. Postglacial trends in palynological richness in the northern Fennoscandian tree-line area and their ecological interpretation. Holocene 8, 43–53. https://doi.org/10.1191/095968398674096317.

Shannon, C.E., 1948. A mathematical theory of communication. Bell Syst. Tech. J. 27, 379–423. https://doi.org/10.1002/j.1538-7305.1948.tb01338.x.

Shen, C.M., Liu, K.B., Tang, L.Y., et al., 2006. Quantitative relationships between modern pollen rain and climate in the Tibetan Plateau. Rev. Palaeobot. Palynol. 140, 61–77. https://doi.org/10.1016/j.revpalbo.2006.03.001.

Simberloff, D., 1972. Properties of the rarefaction diversity measurement. Am. Nat. 106, 414–418. https://doi.org/10.1086/282781.

Simpson, E.H., 1949. Measurement of diversity. Nature 688, 163. https://doi.org/10.1038/163688a0.

Song, W.Q., Li, Y.C., Luo, A., et al., 2024. Historical and contemporary climate jointly determine angiosperm plant diversity patterns across east Eurasia. Ecography 2024, e07062. https://doi.org/10.1111/ecog.07062.

Spicer, R.A., Farnsworth, A., Su, T., 2020. Cenozoic topography, monsoons and biodiversity conservation within the Tibetan Region: an evolving story. Plant Divers. 42, 229–254. https://doi.org/10.1016/j.pld.2020.06.011.

Spicer, R.A., Wolfe, J.A., 1987. Plant taphonomy of late Holocene deposits in trinity (Clair Engle) lake, northern California. Paleobiology 13, 227–245. https://doi.org/10.1017/S0094837300008770.

Su, Y.Q., Zhang, Y., Jia, X.R., et al., 2017. Application of several diversity indexes in forest community analysis. Ecol. Sci. 36, 132–138. https://doi.org/10.14108/j.cnki.1008-8873.2017.01.018.

Sun, X.J., Wang, P.X., 2005. How old is the Asian monsoon system?—palaeobotanical records from China. Palaeogeogr. Palaeoclimatol. Palaeoecol. 222, 181–222. https://doi.org/10.1016/j.palaeo.2005.03.005.

Taylor, L.R., 1978. Bates, Williams, Hutchinson - a variety of diversities. In: Mound, L.A., Waloff, N. (Eds.), The Diversity of Insect Faunas (Symposium of the Royal Entomological Society No. 9). Blackwell Scientific Publishing, Oxford, pp. 1–18.

Valsecchi, V., Carraro, G., Conedera, M., et al., 2010. Late-Holocene vegetation and land-use dynamics in the Southern Alps (Switzerland) as a basis for nature protection and forest management. Holocene 20, 483–495. https://doi.org/10.1177/0959683609355178.

Van der Walt, S., Schönberger, J.L., Nunez-Iglesias, J., et al., 2014. scikit-image: image processing in Python. PeerJ 2, e453. https://doi.org/10.7717/peerj.453.

Veski, S., Koppel, K., Poska, A., 2005. Integrated palaeoecological and historical data in the service of fine-resolution land use and ecological change assessment during the last 1000 years in Rõuge, southern Estonia. J. Biogeogr. 32, 1473–1488. https://doi.org/10.1111/j.1365-2699.2005.01290.x.

Wang, N.N., Liu, L.N., Zhang, Y.R., et al., 2022. A modern pollen data set for the forest—meadow—steppe ecotone from the Tibetan Plateau and its potential use in past vegetation reconstruction. Boreas 51, 847–858. https://doi.org/10.1111/bor.12589.

Wang, Z., Bovik, A.C., Sheikh, H.R., et al., 2004. Image quality assessment: from error visibility to structural similarity. IEEE Trans. Image Process. 13, 600–612. https://doi.org/10.1109/TIP.2003.819861.

Wang, Z.H., Fang, J.Y., Tang, Z.Y., et al., 2011. Patterns, determinants and models of woody plant diversity in China. Proc. R. Soc. B-Biol. Sci. 278, 2122–2132. https://doi.org/10.1098/rspb.2010.2329.

Wei, H.C., Ma, H.Z., Zheng, Z., et al., 2011. Modern pollen assemblages of surface samples and their relationships to vegetation and climate in the northeastern Qinghai-Tibet Plateau, China. Rev. Palaeobot. Palynol. 163, 237–246. https://doi.org/10.1016/j.revpalbo.2010.10.011.

Weng, C.Y., Hooghiemstra, H., Duivenvoorden, J.F., 2006. Challenges in estimating past plant diversity from fossil pollen data: statistical assessment, problems, and possible solutions. Divers. Distrib. 12, 310–318. https://doi.org/10.1111/j.1365-2699.2006.00238.x.

Willis, K.J., Bailey, R.M., Bhagwat, S.A., et al., 2010. Biodiversity baselines, thresholds and resilience: testing predictions and assumptions using palaeoecological data. Trends Ecol. Evol. 25, 583–591. https://doi.org/10.1016/j.tree.2010.07.006.

Winfield, M.O., Lu, C., Wilson, I.D., et al., 2010. Plant responses to cold: transcriptome analysis of wheat. Plant Biotechnol. J. 8, 749–771. https://doi.org/10.1111/j.1467-7652.2010.00536.x.

Woodward, F.I., Williams, B.G., 1987. Climate and plant distribution at global and local scales. Vegetatio 69, 189–197. https://doi.org/10.1007/BF00038700.

Wu, F.L., Fang, X.M., An, C.R., et al., 2013. Over-representation of Picea pollen induced by water transport in arid regions. Quat. Int. 298, 134–140. https://doi.org/10.1016/j.quaint.2012.11.026.

Wu, F.L., Gao, S.J., Tang, F.J., et al., 2019. A late Miocene-early Pleistocene palynological record and its climatic and tectonic implications for the Yunnan Plateau, China. Palaeogeogr. Palaeoclimatol. Palaeoecol. 530, 190–199. https://doi.org/10.1016/j.palaeo.2019.05.037.

Wu, F.L., Fang, X.M., Yang, Y.B., et al., 2022. Reorganization of Asian climate in relation to Tibetan Plateau uplift. Nat. Rev. Earth Environ. 3, 684–700. https://doi.org/10.1038/s43017-022-00331-7.

Xia, J., Ni, J., 2024. Regional features of pollen R-values in China. Sci. China Earth Sci. 67, 295–308. https://doi.org/10.1007/s11430-022-1191-8.

Xiao, X.Y., Shen, J., Wang, S.M., et al., 2008. The plant diversity and its relationship with paleoenvironment since 2.78 Ma revealed by pollen records in the Heqing deep drilling core. Chin. Sci. Bull. 53, 3686–3698. https://doi.org/10.1007/s11434-008-0482-6.

Xiao, X.Y., Zhao, Y., Chi, C.T., et al., 2023. Quantitative pollen-based paleoclimate reconstructions for the past 18.5 ka in southwestern Yunnan Province, China. Global Planet. Change 230, 104288. https://doi.org/10.1016/j.gloplacha.2023.104288.

Xu, Q.H., Cao, X.Y., Tian, F., et al., 2014. Relative pollen productivities of typical steppe species in northern China and their potential in past vegetation reconstruction. Sci. China Earth Sci. 57, 1254–1266. https://doi.org/10.1007/s11430-013-4738-7.

Zhang, L.B., Gilbert, M.G., 2015. Comparison of classifications of vascular plants of China. Taxon 64, 17–26. https://doi.org/10.12705/641.23.

Zhang, R., Tian, F., Xu, Q.H., et al., 2020. Representation of modern pollen assemblage to vertical variations of vegetation and climate in the Yadong area, eastern Himalaya. Quat. Int. 536, 45–51. https://doi.org/10.1016/j.quaint.2019.11.036.

Zhang, Y.X., Steiner, A.L., 2022. Projected climate-driven changes in pollen emission season length and magnitude over the continental United States. Nat. Commun. 13, 1234. https://doi.org/10.1038/s41467-022-28764-0.

Zhang, J.P., Jiang, L.P., Yu, L.P., et al., 2024. Rice's trajectory from wild to domesticated in East Asia. Science 384, 901–906. https://doi.org/10.1126/science.ade4487.

Zhao, Y.J., Zhao, L.N., Hu, H.H., et al., 2023. Angiosperm diversity and conservation progress in China. Chin. J. Nat. 45, 399–409. https://doi.org/10.3969/j.issn.0253-9608.2023.06.001.

Zhao, Y., Tzedakis, P.C., Li, Q., et al., 2020. Evolution of vegetation and climate variability on the Tibetan Plateau over the past 1.74 million years. Sci. Adv. 6, eaay6193. https://doi.org/10.1126/sciadv.aay6193.

Zhou, A.M., Liu, E.H., Li, H., et al., 2018. PsCor413pm2, a plasma membrane-localized, cold-regulated protein from Phlox subulata, confers low temperature tolerance in Arabidopsis. Int. J. Mol. Sci. 19, 2579. https://doi.org/10.3390/ijms19092579.

Zhou, Z.K., Liu, J., Chen, L.L., et al., 2023. Cenozoic plants from Tibet: an extraordinary decade of discovery, understanding and implications. Sci. China Earth Sci. 66, 205–226. https://doi.org/10.1007/s11430-022-9980-9.

Zu, K.L., Chen, F.S., Li, Y.Q., et al., 2024. Climate change impacts flowering phenology in Gongga Mountains, Southwest China. Plant Divers. 46, 774–782. https://doi.org/10.1016/j.pld.2023.07.007.